Developmental Biology 472 (2021) 115–124

Contents lists available at ScienceDirect

Developmental Biology

journal homepage: www.elsevier.com/locate/developmentalbiology

Early patterning of ABCB, ABCC, and ABCG transporters establishes unique territories of small molecule transport in embryonic mesoderm and endoderm

Catherine S. Schrankel, Amro Hamdoun *

Center for Marine Biotechnology and Biomedicine, Scripps Institution of Oceanography, University of California San Diego. 9500 Gilman Drive, La Jolla, CA, 92093-0202, USA

ARTICLE INFO

Keywords:
ABC transporters
MRP
Gut development
Mesoderm signaling
Small molecule
Sea urchin

ABSTRACT

Directed intercellular movement of diverse small molecules, including metabolites, signal molecules and xenobiotics, is a key feature of multicellularity. Networks of small molecule transporters (SMTs), including several ATP Binding Cassette (ABC) transporters, are central to this process. While small molecule transporters are well described in differentiated organs, little is known about their patterns of expression in early embryogenesis. Here we report the pattern of ABC-type SMT expression and activity during the early development of sea urchins. Of the six major ABCs in this embryo (*ABCB1, -B4, -C1, -C4, -C5* and *-G2*), three expression patterns were observed: 1) *ABCB1* and *ABCC1* are first expressed ubiquitously, and then become enriched in endoderm and ectoderm-derived structures. 2) *ABCC4* and *ABCC5* are restricted to a ring of mesoderm in the blastula and *ABCC4* is later expressed in the coelomic pouches, the embryonic niche of the primordial germ cells. 3) *ABCB4* and *ABCG2* are expressed exclusively in endoderm-fated cells. Assays with fluorescent substrates and inhibitors of transporters revealed a ring of ABCC4 efflux activity emanating from *ABCC4*$^{+}$ mesodermal cells. Similarly, ABCB1 and ABCB4 efflux activity was observed in the developing gut, prior to the onset of feeding. This study reveals the early establishment of unique territories of small molecule transport during embryogenesis. A pattern of *ABCC4/C5* expression is consistent with signaling functions during gut invagination and germ line development, while a later pattern of *ABCB1/B4* and *ABCG2* is consistent with roles in the embryonic gut. This work provides a conceptual framework with which to examine the function and evolution of SMT networks and to define the specific developmental pathways that drive the expression of these genes.

1. Introduction

A core feature of multicellularity is the precisely regulated movement of small molecules between cells (Babonis and Martindale, 2017; Titus and Goodson, 2018). Regulation of small molecule movement is central to signaling, metabolic homeostasis and interaction with the external environment. Small molecule transporters (SMTs) are key regulators of uptake and efflux. In adult organisms, SMTs are distributed among tissues and connected through the circulation in a coordinated process termed remote sensing and signaling (Nigam, 2015; Rosenthal et al., 2019; Ahn and Nigam, 2009). In embryos and stem cells, regulation of specific metabolites and small molecules drives cell fate and function (Onjiko et al., 2015; Yanes et al., 2010; Butcher, 2017; Helker et al., 2019), but the associated patterns of SMT expression (Shipp and Hamdoun, 2012; Zúñiga et al., 2009; Engelhart et al., 2020) are not fully described.

A major set of SMTs belongs to the ATP-binding cassette (ABC) or Solute Carrier (SLC) families (Dean, 2001; Almén et al., 2009). These membrane protein families include a variety of uptake and efflux transporters that handle diverse small molecule ligands important for development. Many of these proteins, such as ABCB1 and ABCC1, have been extensively studied in association with xenobiotic and endobiotic transport, as well as variable drug absorption and disposition along the gastrointestinal tract (Szakács et al., 2008; Müller et al., 2017). Upregulation of these genes is also responsible for acquired chemotherapy resistance in cancers (Chen and Tiwari, 2011). However, in addition to effluxing drugs, it is now appreciated that these and other ABC transporters contribute to disease by transporting signaling molecules that

* Corresponding author.
E-mail address: ahamdoun@ucsd.edu (A. Hamdoun).

https://doi.org/10.1016/j.ydbio.2020.12.021
Received 10 July 2020; Received in revised form 8 December 2020; Accepted 22 December 2020
Available online 15 January 2021

govern migratory and morphogenetic behaviors of cells (Fletcher et al., 2010; Jin et al., 2014; Cole, 2014; Hannun and Obeid, 2008; Randolph et al., 1998).

Several transporters play important endogenous signaling roles in development. Examples include transporters in auxin-mediated root guidance (Robert and Friml, 2009), slime mold stalk development (Miranda et al., 2015), nematode diapause (Yabe et al., 2005), ciliogenesis in zebrafish (Jin et al., 2014), germ cell chemoattraction in flies and ascidians (Ricardo and Lehmann, 2009; Deshpande et al., 2016; Kassmer et al., 2015, 2020), and hindgut invagination in the sea urchin (Shipp et al., 2015). However, to date, few studies have characterized the spatial and temporal patterns of transporter networks during development. This is important to understand, because embryos express multiple transporters simultaneously, many of which have overlapping substrates that can act in concert to regulate signal and metabolite distribution (Giacomini et al., 2010).

The sea urchin embryo provides a powerful system for understanding the regulation and activity of transporters across developmental stages. Embryogenesis is highly synchronous and utilizes a limited number of cells. Germ layers are specified within the first 24 h of development, and endomesoderm differentiation has been mapped experimentally at the gene regulatory network (GRN) level (Davidson et al., 2002). The embryo develops a gut tube by 48 h post-fertilization (hpf), which becomes morphologically compartmentalized by 72 hpf (Peter and Davidson, 2011; Annunziata et al., 2014). Larval feeding can start by 3 days post-fertilization (dpf), and most digestion and adsorption occurs in the stomach (Burke, 1981; Annunziata et al., 2019).

The sea urchin is the best characterized embryo model for the study of ABC transporters, with a robust foundation of knowledge on transporter expression. In the first 72 h of embryogenesis, transcripts of several important members of the *ABCB, ABCC* and *ABCG* subfamilies are differentially regulated (Shipp and Hamdoun, 2012; Tu et al., 2014). These include *ABCB1* which is active in protecting early embryos (Hamdoun et al., 2004; Bošnjak et al., 2009), *ABCG11* which is expressed in pigment cells (Perillo et al., 2020), and *ABCC5* which is also expressed in pigment cells and contributes to proper gut development (Shipp et al., 2015). In addition, specific fluorescent substrates have been characterized for each subfamily (Gökirmak et al., 2012, 2014), which enables *in-vivo* tracking of transporter-mediated efflux activity.

Here, we describe the spatial expression domains of homologs of *ABCB1, ABCB4, ABCC1, ABCC4,* and *ABCG2* using whole mount *in-situ* hybridization. We adapted live-cell transport and inhibition assays to determine how differential expression leads to distinct regions of active transport during key stages of embryogenesis. The results reveal unexpected compartmentalization of gene expression and protein activity of ABC transporters along regions of early mesoderm and differentiating endoderm. This map of transport has implications for signaling, metabolism, and embryonic protection. Our observations provide a novel conceptual framework for studying the regulation, function, and evolution of SMT networks across animal development.

2. Materials and methods

2.1. Spawning, culturing and feeding

Purple sea urchins, *Strongylocentrotus purpuratus*, were collected at San Diego, California and housed in aquaria with running filtered seawater at 12 °C. Adults were fed *Macrocystis pyrifera*. Animals were spawned, fertilized, and embryos cultured in 0.22 μM filtered seawater (FSW) at 15 °C.

2.2. Probe generation for whole mount in-situ hybridization (WMISH)

Templates for WMISH probes were generated from PCS2+8 plasmids containing full-length coding sequences of transporter genes *ABCB1a, ABCB4a, ABCC1a, ABCC4a,* and *ABCG2a* (Gökirmak et al., 2012). Primers are listed in Supplemental Table 1. Primer pairs had a T7 promoter site incorporated into either the forward (for sense probe transcription) or reverse primer (for antisense probe transcription). Probe templates of ~900–1500 bp were amplified from plasmids using Phusion High-Fidelity DNA polymerase (NEB) and cleaned by PCR-column purification (Qiagen). RNA probes were transcribed with T7 synthesis and digoxigenin (DIG) or Fluorescein-labeling kits (Roche, Indianapolis, IN) according to manufacturer protocols.

2.3. Whole-mount in-situ hybridization

WMISH was performed as previously described (Shipp and Hamdoun, 2012) with minor modifications. Briefly, embryos were fixed in a 4% paraformaldehyde EPPES buffer overnight at 4 °C and stored long-term in 100% methanol. Embryos were washed several times through Tris-buffered saline + Tween-20 (TBST: 100 mM Tris pH 7.5, 150 mM NaCl, 0.1% Tween-20) and transferred into a pre-hybridization buffer (HB: 50% formamide, 5X saline-sodium citrate [SSC], 5 mM EDTA, 0.1% Tween-20, 2X Denhardt's Solution, 50 μg/mL heparin, 500 μg/mL yeast tRNA) in several steps (30% HB-TBST, 60% HB-TBST, and 100% HB). Embryos were pre-hybridized in HB for 1 h at 62 °C. Probes were hybridized overnight at 62 °C, at a final probe concentration of 0.5–1 ng/μL. Samples were washed through SSC and TBST buffers for several hours, blocked in 10% sheep serum with BSA for 1 h (SS/BSA), and incubated with anti-DIG-AP antibody (1:1500; Roche, Indianapolis, IN) in 5% SS/BSA overnight at 4 °C. Colorimetric alkaline-phosphatase (AP) staining was performed using NBT/BCIP (Sigma) in filtered AP Buffer (100 mM Tris 9.5, 100 mM NaCl, 50 mM $MgCl_2$, 1 mM Levamisole, 0.1% Tween, 10% DMF) for several hours to overnight, depending on the probe. Double colorimetric *in-situ* staining was performed using FastRed stain (Sigma-Aldrich). Stained embryos were imaged on a Zeiss AxioImager M2 microscope using a 20X Apochromat 0.9 NA air objective and Axiocam 506 color camera.

Double fluorescent *in-situ* (FISH) staining was performed using POD-conjugated anti-Fluorescein and anti-DIG antibodies (1:1500; Roche, Indianapolis, IN) and TSA amplification with Cy-3 and Cy-5 (1:400, Akoya Biosciences) as previously described (Shipp et al., 2015). FISH-stained embryos were counterstained with DAPI and imaged on a Zeiss LSM 700 laser scanning confocal microscope using a 20x Plan-Apo 0.8 NA air objective.

2.4. In-vivo transporter dye efflux assays on tagged embryos

Transporter substrate assays: To assess where ABC transporter subfamilies are active in different tissues during development, live-cell efflux assays using fluorescent substrates and inhibitors (Gökirmak et al., 2012, 2014) were optimized across different developmental stages (Fig. S3). Fertilized eggs were first injected with $LCK^{mCherry}$ or $H2B^{CFP}$ mRNA constructs (75 ng/μL) in order to visualize membrane or nuclei features during accumulation assays, which do not alter signal accumulation patters ((Gökirmak et al., 2012); Fig. S4). The relative amount of substrate accumulation within tissues is used as a proxy for transporter activity. To observe ABCC1 and ABCC4 efflux activity, embryos were incubated with fluorescein diacetate (FDA; Sigma-Aldrich) at a final concentration of 20 nM at 15 °C for 60 min in the dark. Embryos were washed six times with FSW after incubation and recovered for 30 min in the dark before imaging. For ABCC4-specific inhibitor assays, embryos were co-incubated with 10 μM Ceefourin1 or 2 (Abcam) along with the FDA. To assess ABCB1 and ABCB4 efflux activity, embryos were incubated with BODIPY-verapamil (B-ver, Invitrogen) in FSW at a final concentration of 50 nM at 15 °C for 60 min in the dark. Embryos were washed three times with FSW and immediately imaged. For ABCB-specific inhibitor assays, embryos were co-incubated in 1 μM PSC833 (Sigma-Aldrich) along with the B-ver substrate. All substrates and inhibitors were rehydrated into 1000X stock solutions with dimethyl sulfoxide (DMSO) and stored at −20 °C. All stocks were diluted such that

the final DMSO concentration did not exceed 0.15%.

Imaging: Embryos were imaged on a Zeiss LSM 700 laser scanning confocal microscope using a 20x Plan-Apo 0.8 NA air objective. Images were obtained using optical sectioning and multi-position acquisition settings in ZEN software (Carl Zeiss Microscopy GmbH). For high quality representative micrographs, some embryos were imaged on a Leica TCS SP8 laser scanning confocal microscope (20x objective, NA 0.8), equipped with the Lightning deconvolution module (Leica Microsystems GmbH). All embryos exposed to the same substrate or substrate + inhibitor were imaged with identical confocal settings (pinhole size, gain, laser power, zoom, and scan speed). Z-stack slices were acquired at 0.2 μm thickness (Lightning modules) or 1.5 μm thickness (substrate accumulation analysis). 3D reconstruction of confocal stacks into video format was performed with Imaris Software (Bitplane, Oxford Instruments).

Substrate accumulation analysis: Post-acquisition image analysis was performed using ImageJ software (Schindelin et al., 2012). The relative efflux activity of each transporter was quantified by measuring the intracellular substrate fluorescence intensity per pixel in specific regions using the 'Measure' module of ImageJ. Measurements were made from single-plane, equatorial confocal sections of embryos in which the mesoderm (blastulae), coelomic pouches and foregut (gastrulae), or stomach (larvae) were in maximum focus for the developmental stage in question. Mean raw intensity measurements were compared across tissues within control embryos, or between control and inhibited embryos. To calculate the mean fold change in accumulation relative to controls, raw fluorescence intensity values of each individual inhibited embryo were divided by the mean of the raw intensity values of the wildtype (WT) control embryos. Fold changes in accumulation were determined from raw intensity measurements of several embryos ($n > 6$) pooled from at least three experimental batches and tested by 1-way ANOVA analysis with Bonferroni's multiple comparisons correction, blocked by batch.

3. Results

3.1. ABCC1 is expressed ubiquitously while ABCC4 is localized to non-skeletal mesoderm and the embryonic germ cell niche

In addition to xenobiotics, ABCC transporters handle a wide range of developmental signaling molecules such as cyclic nucleotides, sphingolipids, leukotrienes, and eicosanoids (Jin et al., 2014; Cole, 2014; van Aubel, 2002; Wen et al., 2015). *In-situ* hybridization in the sea urchin embryo reveals that *ABCC1* mRNA is present in the unfertilized egg (Fig. 1A; Control sense probes shown in Fig. S1). It is ubiquitously expressed through blastula stages (Fig. 1B and C) and early gastrulation (Fig. 1D). During gastrulation (Fig. 1E and F), transcripts further accumulate in the apical plate, a specialized region of neuroepithelium that develops into an innervated larval sensory structure called the apical organ (Angerer et al., 2011). At the early pluteus larval stage (Fig. 1G), *ABCC1* expression becomes enriched in the sensory ciliary band as well as the stomach.

In contrast, *ABCC4* develops a more restricted pattern in the mesoderm and its derivatives (Fig. 1H–S). *ABCC4* expression is first evident at low levels throughout the egg and early blastula stages (Fig. 1, H and I). Transcripts accumulate in the non-skeletal mesoderm (NSM) of blastulae and early gastrulae (Fig. 1J and K). *ABCC4* remains present at the tip of the archenteron during gastrulation (Fig. 1L) and continues to accumulate in the coelomic pouches at both the prism and pluteus larval stages (Fig. 1, M and N). The coelomic pouches provide the embryonic niche for primordial germ cells (PGCs), which will seed the adult with egg or

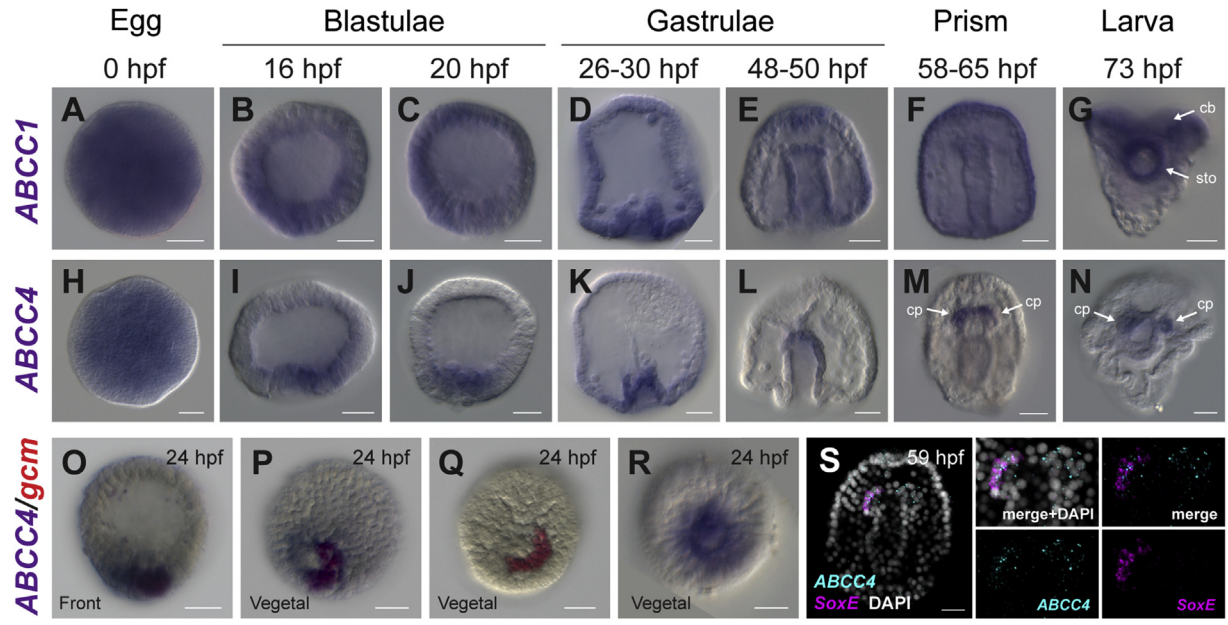

Fig. 1. *ABCC1* is broadly expressed and *ABCC4* genes are differentially expressed in the mesoderm and coelomic pouches throughout embryogenesis. *ABCC1* and *ABCC4* transporter transcripts were visualized by whole mount *in situ* hybridization. The name of each hybridized gene is shown on the left, and developmental time (hours post fertilization, hpf) and stages are indicated at the top. **(A–G) *ABCC1* is broadly expressed across development and becomes enriched in the stomach.** The diffuse global staining of *ABCC1* indicates ubiquitous constitutive expression in the egg and throughout development up to the gastrula stage (**A-E**). Additional transcript accumulation is present in the apical plate of gastrulae (**E**). By the larval stage (**G**), *ABCC1* transcripts also accumulate in the stomach (sto) and the ciliary band (cb). **(H–N) *ABCC4* is expressed in early mesoderm and coelomic pouches**. *ABCC4* is present in the egg (**H**) and becomes enriched in the early mesoderm at the vegetal plate of blastulae (**I–J**) and the tip of the archenteron of gastrulae (**K–L**). During prism to larval stages (**M-N**), *ABCC4* is localized in both the coelomic pouches (cp). **(O–S) *ABCC4* co-localizes with markers of the non-skeletal mesoderm (NSM) and coelomic pouches.** *ABCC4* expression is present in the ring of NSM and overlaps with *gcm*, a marker for aboral mesoderm **(O–P)**, but is not localized in the small micromeres located at the vegetal pole of the blastula (**P, R**). Single stains are shown for *gcm* (**Q,** vegetal view) and *ABCC4* (**R,** vegetal view). During late-gastrulation, *ABCC4* (cyan) is co-expressed with *SoxE* (magenta), a marker for coelomic pouch cells (**S**). *ABCC4* is present throughout both coelomic pouches, whereas *SoxE* is restricted to the left pouch (**S**, 59 hpf insets). All animals in panels **A-O** and **S** are oriented as front view. Images in **S** are maximum projections of several merged confocal stacks. Scale bars, 20 μM.

sperm stem cells (Pehrson and Cohen, 1986; Juliano et al., 2006, 2010). The PGCs of the sea urchin are specified from small micromeres that appear at the 5th cleavage and sit at the vegetal pole of the blastula until they migrate to the archenteron tip during gastrulation (Campanale et al., 2014).

Because the expression pattern of *ABCC4* mirrors that of many mesodermal, small micromere, and coelomic pouch-specific markers, we co-stained with *gcm*, a marker for aboral mesoderm (Ransick et al., 2002), and *SoxE* (Fig. 1O–S), a marker for coelomic pouch precursors and the left coelomic pouch (Materna et al., 2013; Luo and Su, 2012). At the mesenchyme blastula stage (24 hpf), *ABCC4* expression is present in the entire ring of NSM and is absent from the small micromeres located at the center of the vegetal plate (Fig. 1O and P). *ABCC4* is expressed throughout both oral and aboral mesoderm, compared to *gcm* alone (Fig. 1Q and R). By late gastrulation (59 hpf; Fig. 1S), *ABCC4* transcripts are present in both the coelomic pouches, whereas *SoxE* is restricted to the left pouch (Fig. 1S, insets; Fig. S2A).

3.2. *ABCC4-specific efflux activity is restricted to the early mesoderm and the coelomic pouches*

Next, we assayed the efflux of fluorescent substrates of the ABCC transporters (Fig. 2). In these assays, live embryos are incubated with an ABCC-specific substrate (fluorescein-diacetate, FDA) that is effluxed by the transporter (Shipp et al., 2015; Gökirmak et al., 2012, 2014) (Fig. S3). In regions of high transporter activity, the fluorescent compound is effluxed from cells and the region remains dark. In regions of low (or pharmacologically inhibited) transporter activity, the substrate accumulates and the areas become brightly fluorescent.

In late blastulae, the ectodermal and primary mesenchyme (skeletal) cells quickly saturate with FDA (Fig. 2A). In contrast, the NSM exhibits significantly less FDA signal than the ectoderm (Fig. 2A–i), indicative of high efflux activity (Table 1, $p < 0.0001$). Blastulae consistently exhibit a 3.65-fold mean change in FDA accumulation between the ectoderm and the NSM (Table 1, $p < 0.0001$; Fig. S4A).

Three-dimensional projections of blastulae show a torus of cells with high efflux activity, overlapping with the expected location of the ring of NSM surrounding the small micromeres (Video 1). This torus includes clusters of wedge-shaped "bottle cells" (Nakajima and Burke, 1996) within the mesoderm. The small micromeres, which are inside of this ring, do not appear to have high levels of efflux activity at this stage, as evidenced by their accumulation of FDA (Fig. 2A–i; Fig. S4A).

Supplementary video related to this article can be found at https://doi.org/10.1016/j.ydbio.2020.12.021.

Because *ABCC4* mRNA is expressed in the NSM cells similar to those that are low in FDA accumulation (Fig. 1, O-R), we next examined whether inhibitors of ABCC4 (Cheung et al., 2014) would alter the observed FDA pattern. Consistent with the notion that the mesodermal ring of low FDA accumulation is mediated by ABCC4, exposure to both Ceefourin1 (CF1, 10 μM) and Ceefourin2 (CF2, 10 μM) results in stronger FDA signal in this territory (Fig. 2A–ii; Fig. S4A). The NSM of CF2-inhibited embryos accumulates 2.58-fold greater mean levels of FDA signal compared to WT embryos (Table 2, $p < 0.0001$). Similar increases were noted for CF1 exposure (Table 2, $p < 0.0001$; Fig. S4A).

Next we tested gastrulae for the presence of ABCC4 efflux activity in the coelomic pouches (Fig. 2B; Fig. S4B). In WT embryos, FDA signal accumulates at significantly lower levels in the coelomic pouches and foregut region, compared to the adjacent midgut tissue (Fig. 2B). When compared across multiple independent batches, the coelomic pouches accumulate almost 5-fold less substrate than the midgut (Table 1, $p = 0.0004$). Similar to the earlier NSM field, FDA re-accumulates in areas of high *ABCC4* expression after co-incubation with the inhibitor CF2 (Fig. 2B–ii). On average the CP-localized FDA signal increases 2-fold under ABCC4 inhibition (Table 2, $p < 0.0001$). Importantly, ectodermal FDA accumulation was not significantly affected under CF2 exposure at the gastrula stage (Table 2, $p = 0.4717$), indicating that the inhibitors were primarily acting in regions with highest localized *ABCC4* expression. Together these *in situ* and efflux assay data indicate efflux activity in the NSM and coelomic pouch regions is largely derived from ABCC4-mediated transport.

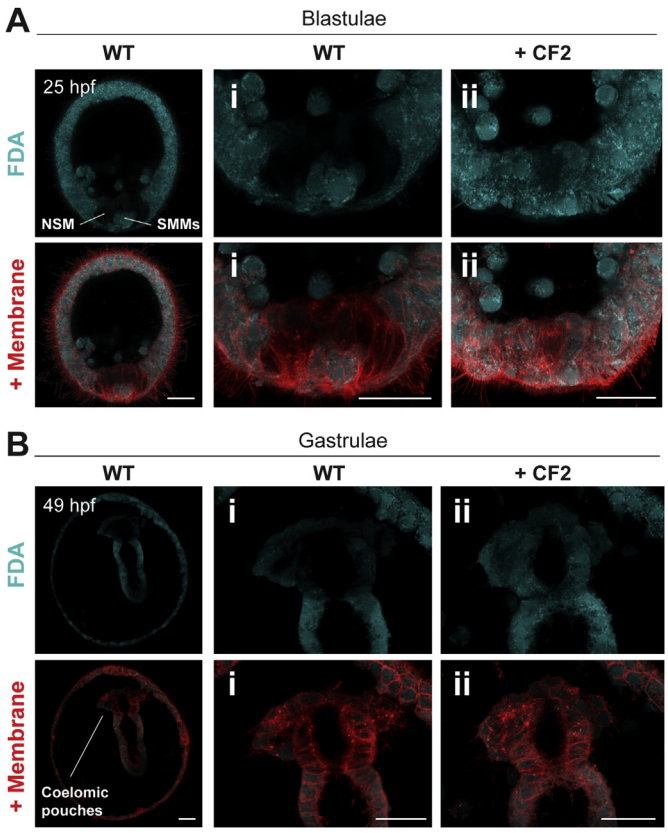

Fig. 2. FDA efflux activity mirrors *ABCC4* mRNA expression domains in blastulae and gastrulae. Membrane-tagged embryos were incubated with fluorescent substrates specific to ABCC transporters (fluorescein diacetate, FDA (Shipp et al., 2015; Gökirmak et al., 2014; Gökirmak et al., 2012);). Regions with high transporter activity remain dark, whereas regions with brighter intracellular signal indicate lower substrate efflux. ABCC4 transporter activity can be blocked with Ceefourin2 (CF2 (Cheung et al., 2014);). **(A) A ring of mesoderm in blastulae exhibits significant FDA efflux activity.** FDA accumulates at lower levels in the non-skeletal mesoderm (NSM) compared to the surrounding ectoderm and the small micromeres (SMMs, future primordial germ cells) located at the vegetal pole. Insets (**i-ii**) show magnification of the vegetal plate. Efflux of FDA is abrogated by co-incubation with CF2 (**ii**; 10 μM). **(B) Efflux activity in the coelomic pouches is sensitive to ABCC4-specific inhibition.** FDA assays were performed on membrane-tagged gastrulae. Insets **(i-ii)** show magnification of the foregut and coelomic pouch region. FDA accumulates at low levels in control WT pouches compared to the rest of the gut. FDA re-accumulates in this region after co-incubation with CF2 (10 μM). All images in **A** and **C** are maximum intensity projections of several 0.2 μM confocal stacks around the equatorial plane. Membrane overlay is shown in the bottom panels. Scale bars, 20 μM. CPs, coelomic pouches and foregut region. Hpf, hours post-fertilization. Images are representative of embryos from at least three independent mate pairs (Tables 1 and 2). Representative single-plane confocal slices are shown in Fig. S4.

3.3. *ABCB and ABCG transporters become enriched in hindgut and midgut-fated tissues*

Next, we investigated expression domains of ABCB and ABCG subfamilies, which often perform protective functions against xenobiotics (Szakács et al., 2008; Müller et al., 2017). Consistent with previous reports (Shipp and Hamdoun, 2012), *ABCB1* is expressed during oogenesis and remains ubiquitous throughout early gastrula stages (Fig. 3A–D). By

Table 1
Fluorescent substrate accumulation patterns.

Substrate	Time	Tissue	Mean fold-change in accumulation	*P* value	N
FDA	24-27 hpf	Ectoderm vs NSM	3.646 ± 0.293	$p < 0.0001$	n = 37 from 5 females
	50-54 hpf	Midgut vs CPs/Foregut	4.997 ± 0.375	$p < 0.0001$	n = 31 from 4 females
B-ver	70-73 hpf	Ectoderm vs Midgut	4.227 ± 0.307	$p < 0.0001$	n = 44 from 7 females

The mean fold-changes in raw fluorescent intensity values were calculated (±S.E.M) from pooled embryos. Differences between tissues were tested by 1-way ANOVA with Bonferroni's multiple comparisons test on raw fluorescent values, blocked by batch. B-ver, BODIPY-Verapamil. CPs, Coelomic pouches. FDA, fluorescein diacetate. Hpf, hours post-fertilization. NSM, non-skeletal mesoderm.

Table 2
FDA accumulation under ABCC4 inhibition.

Time	Tissue	Inhibitor	Mean fold-change in accumulation	*P* value	n
24-27 hpf	NSM:	CF1	2.575 ± 0.163	****, p<0.0001	n = 38 from 5 females
		CF2	2.312 ± 0.122	****, p<0.0001	n = 32 from 4 females
	Ectoderm:	CF1	1.275 ± 0.069	*, p=0.0262	n = 38 from 5 females
		CF2	1.521 ± 0.129	**; p=0.0053	n = 32 from 4 females
50-54 hpf	CPs/foregut:	CF2	2.040 ± 0.109	****, p<0.0001	n = 23 from 3 females
	Ectoderm:	CF2	1.440 ± 0.092	ns, p=0.4717	n = 23 from 3 females

The mean fold-changes in raw fluorescent intensity values were calculated (±S.E.M) from pooled embryos. Differences between WT and inhibited embryos were tested by 1-way ANOVA with Bonferroni's multiple comparisons test on raw fluorescent values, blocked by batch. CF1, Ceefourin 1. CF2, Ceefourin 2. CPs, coelomic pouches. FDA, fluorescein diacetate. Hpf, hours post-fertilization. NSM, non-skeletal mesoderm.

late gastrulation (Fig. 3E and F), *ABCB1* transcripts accumulate in the blastopore (Fig. S2B), the hindgut (presumptive intestine) and midgut (presumptive stomach). Expression also becomes more localized in the apical plate (Fig. 3E and F). By the early pluteus larval stage (Fig. 3G), *ABCB1* is most enriched in the stomach and the ciliary band.

The closely related *ABCB1* ortholog, *ABCB4*, demonstrates a contrasting pattern of absence in the egg and early stages (Fig. 3H–K), followed by strong expression during gastrulation in the blastopore (Fig. S2B) and hindgut (Fig. 3L). This domain expands to include the midgut and stomach of prism and larval stages, respectively, but not the foregut and coelomic pouches (Fig. 3M and N). *ABCG2* follows a similar expression profile as *ABCB4* (Fig. 3O–U). *ABCG2* transcripts appear relatively low in the egg, blastula stages, and at the onset of gastrulation (Fig. 3O–R). Transcript accumulation first becomes evident in the blastopore (Fig. S2B) and hindgut of late gastrulae (Fig. 3S). The *ABCG2* expression domain expands to the midgut of prism and stomach of larval stages, but is not evident in the foregut or coelomic pouches (Fig. 3T–U). Co-expression of *ABCB1, ABCB4* and *ABCG2* occurs across the endodermal tissue, and is further concentrated in some presumptive stomach cells at the gastrula and larval stage (Fig. 3V–W).

3.4. Transport of an ABCB substrate in the gut before feeding

To define regions of ABCB-specific active transport in live embryos, we repeated *in-vivo* substrate accumulation assays with the ABCB1 and ABCB4-specific substrate BODIPY-verapamil (B-ver) and inhibitor PSC833 (Fig. S3; Fig. 4). At the blastula stage, ABCB efflux activity is evident across the entire embryo, and co-incubation with the inhibitor causes an increase in B-ver signal accumulation (Fig. 4A). Given that ABCB proteins are expressed in the gut of several animals and that we observed enrichment of *ABCB1* and *ABCB4* transcripts in the hindgut and midgut (Fig. 3), we next examined if the respective efflux activity is more prominent in gastrulae and larvae. At late-gastrula stages (54 hpf, Fig. 4B), the ectoderm accumulates low levels of B-ver signal, and remains sensitive to PSC833 inhibition. However, B-ver signal is not observed in the developing midgut, foregut and coelomic pouches unless embryos are co-incubated with the PSC833 inhibitor (Fig. 4B), indicating a strong endogenous ABCB-specific efflux activity in these regions.

At 70–73 hpf, when larvae exhibit a complete tripartite compartmentalization of esophagus, stomach and intestine, the stomach accumulates significantly less B-ver than the ectoderm (Fig. 4C–D), and to a lesser extent, the foregut region (WT panels, Fig. 4C). The ectoderm accumulates 4.23-fold higher mean levels of B-ver signal than the stomach across multiple independent batches (Table 1, $p < 0.0001$; Fig. S4C). Both stomach and ectodermal B-ver accumulation increase significantly after exposure to PSC833 (Fig. 4C–D, $p < 0.0001$). However, the stomach region shows the greatest increase in accumulation compared to the ectoderm (4.88-fold increase compared to a 3.20-fold increase in mean signal accumulation upon inhibition, respectively; Table 3, $p < 0.0001$).

Overall, transport of the ABCB1 and ABCB4 substrate B-ver is evident in the ectoderm across embryogenesis, becomes enriched in gut compartments of late gastrulae and larvae, and is most sensitive to PSC833 inhibition in gut tissues. These data indicate an enrichment of ABCB-specific protein activity in the gut, in agreement with *ABCB1* and *ABCB4* mRNA expression domains.

4. Discussion

This study is the first to determine maps of the expression of several ABC transporters during deuterostome development (Fig. 5). Transporters are clearly partitioned across germ layers throughout the first 72 h of sea urchin embryogenesis (Table 4). Three features of this pattern are: 1) a strong overlap of *ABCC4* and *ABCC5* expression in the mesoderm, 2) sustained expression of *ABCB1* and *ABCC1* in the ectoderm, and

Table 3
B-ver accumulation under ABCB inhibition.

Time	Tissue	Inhibitor	Mean fold-change in accumulation	*P* value	n
70-73 hpf	Stomach	PSC833	4.878 ± 0.271	****, $p < 0.0001$	n = 31 from 7 females
	Ectoderm	PSC833	3.200 ± 0.095	****, $p < 0.0001$	n = 93 from 9 females

The mean fold-changes in raw fluorescent intensity values were calculated (±S.E.M) from pooled embryos. Differences between WT and inhibited embryos were tested by 1-way ANOVA with Bonferroni's multiple comparisons test on raw fluorescent values, blocked by batch. B-ver, BODIPY-Verapamil. Hpf, hours post-fertilization.

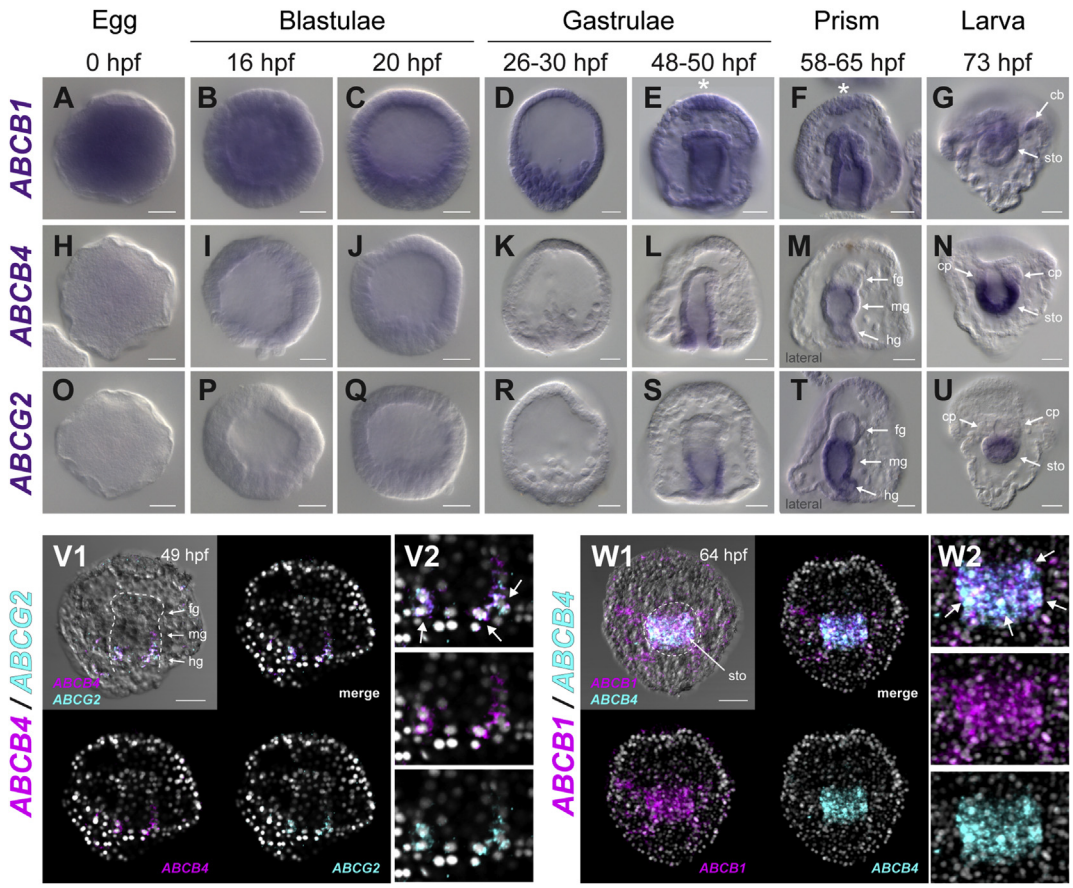

Fig. 3. *ABCB* and *ABCG* transporter genes become enriched in endoderm-fated tissues throughout embryogenesis. *ABCB1, B4,* and *G2* transcripts were visualized with whole mount *in situ* hybridization. The name of each hybridized gene is shown on the left, and developmental time (hours post fertilization, hpf) and stages are indicated at the top. **(A–G) *ABCB1* is ubiquitously expressed and becomes enriched in the gut**. Staining indicates ubiquitous ABCB1 expression throughout development up to the gastrula stage. By late gastrula and prism stages (**E-F**), *ABCB1* becomes enriched in the entire gut tube and in the apical plate (*), the site of a future sensory organ. By larval stage (**G**), *ABCB1* is enriched in the stomach (sto) and faintly in the ciliary band (cb). **(H–U) *ABCB4* and *ABCG2* are exclusively expressed in the gut**. *ABCB4* and *ABCG2* are first expressed at the late gastrula stage (**L, S**) and are only present in the hindgut (hg) and midgut or stomach (mg/sto), but not the foregut (fg) of gastrulae and larvae (**N, U**). Expression is also absent in the coelomic pouches (cp). **(V–W) Co-expression of *ABCB1, ABCB4,* and *ABCG2* in gut tissues.** Double FISH of gastrulae (**V**) and larvae (**W**) are shown, counterstained with DAPI. Examples of stronger co-localization in cells are highlighted with white arrows in gut insets (**V2, W2**). Images in **V–W** are maximum projections of several merged confocal stacks. All animals in **A-W** are oriented as front view, except for **M** and **T** (shown in lateral view). Scale bars, 20 μM.

3) the early emergence of protective transporters *ABCB1, ABCB4,* and *ABCG2* in distinct compartments of the endoderm. Our results also show that ABCC4-specific transport of FDA in living embryos recapitulates the expression domains of *ABCC4*. In contrast, ABCB-specific transport mirrors the gut-specific expression domains of *ABCB1* and *ABCB4*. Collectively, this map of transport overlaps with many key specification and morphogenetic events in the mesoderm, endoderm and ectoderm (Fig. 5).

4.1. Patterns of ABCC4 expression in the mesoderm are associated with primary invagination of the gut and development of the embryonic germ line niche

One of the most interesting patterns we observed in this study was the enrichment of *ABCC4* transcripts and efflux activity from a broad profile post-fertilization, to an NSM-specific domain in blastulae that is later concentrated in the coelomic pouches of larvae (Fig. 5A). Active transport can be a mechanism for the secretion of molecules that act in morphogenesis, either as short-range signals between neighboring cells, or long-range signals that work across larger distances (Müller et al., 2013). Known signaling substrates of ABCC4 and ABCC5 include cyclic nucleotides (Shipp et al., 2015; van Aubel, 2002; Wielinga et al., 2003; Wijnholds et al., 2000), prostaglandins (Jin et al., 2014; Reid et al., 2003), lipid-derived molecules and glucuronide or glutathione (GSH)-conjugated metabolites (Wen et al., 2015; Jedlitschky et al., 1996). In the early phase of its expression domain, *ABCC4* is partially overlapping with *ABCC5,* which is expressed only on one side of the NSM (Shipp et al., 2015). Given these observations, we hypothesize that ABCC4 activity, in concert with ABCC5, may be involved in the export of mesodermal signaling substrates. Notably, strong efflux of FDA is also present in the mesoderm of sea star blastulae (Fig. S5), indicating a potentially conserved role for a transporter signaling center across the 500 million years of evolution spanned by these two species (Wada and Satoh, 1994).

The activity of ABCC4 in the NSM and its derivatives may function in gut differentiation or morphogenesis if exported signals are received by the adjacent endoderm. Lipid derivatives and other small molecules have been shown to drive endoderm development in human embryonic stem cells and zebrafish (Helker et al., 2019; Korostylev et al., 2017; Bogacheva et al., 2018; Chen et al., 2009). In the sea urchin, cAMP may be exported by ABCC5 in nascent pigment cells (derivates of the aboral NSM), and this signal is thought to coordinate late invagination (Shipp et al., 2015). Alternatively, ABCC transporter activity may be relevant for the development or behavior of other NSM cell types, which include immune cells and muscle progenitors (Solek et al., 2013; Schrankel et al., 2016; Andrikou et al., 2013, 2015).

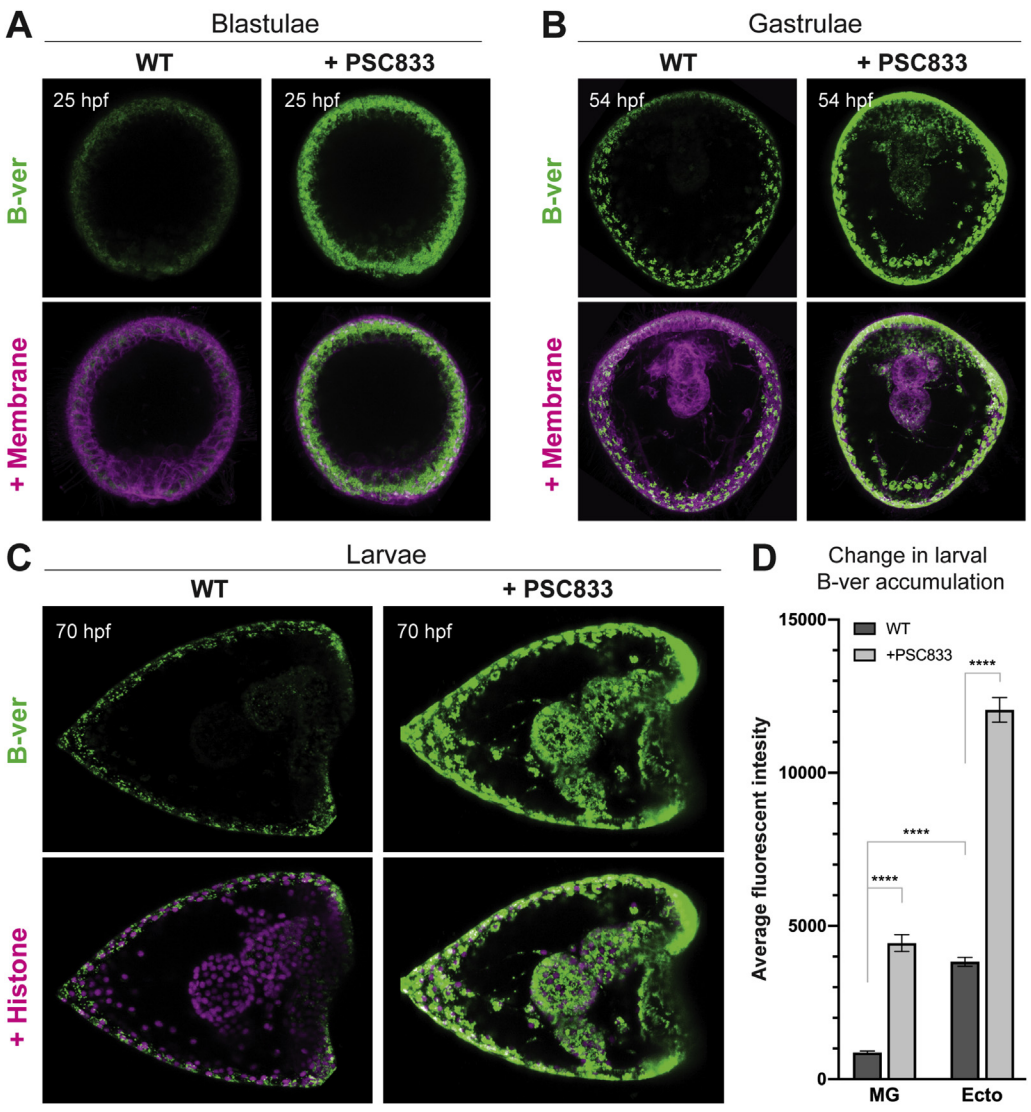

Fig. 4. ABCB-specific activity is present throughout development and becomes enriched in gut tissues in prism and pluteus larvae. Membrane or histone-tagged embryos were incubated with fluorescent substrates that are specific to ABCB transporters (BODIPY-verapamil, B-ver). Transporter activity can be blocked with the ABCB-specific inhibitor PSC833 (Gökirmak et al., 2012). **(A) Blastulae exhibit global ABCB transporter activity.** B-ver accumulates at low levels throughout wildtype (WT) blastulae, compared to ABCB-inhibited embryos (PSC833; 1 μM), indicating global ABCB efflux activity at this stage. **(B–C) The stomach, intestine, and coelomic pouches exhibit the highest ABCB-specific efflux activity in gastrulae and larvae.** B-ver accumulates at low levels in WT guts compared to the ectoderm of gastrulae **(B)** and larvae **(C)**. Efflux of B-ver across all tissues can be abrogated by co-incubation with PSC833 (1 μM). **(D) Quantification of B-ver accumulation.** Mean raw intensity measurements (±S.E.M) were compared across WT and PSC833-inhibited larvae. Differences between WT and inhibited embryos were tested by 1-way ANOVA with Bonferroni's multiple comparisons test on raw fluorescent values, blocked by batch (****, $p < 0.0001$; n = 31–93 pooled from 7 females). All images in **A-C** are maximum intensity projections of several 1.5 μM confocal stacks around the equatorial plane; membrane or histone overlay is shown in the bottom panels. All animals in **A-B** are oriented as front view, and the larval stage (**C**) is shown in lateral view. Scale bars, 20 μM. Ecto, ectoderm. Hpf, hours post-fertilization. MG, midgut (stomach). Images are representative of embryos from at least three independent mate pairs (Tables 1 and 3; Fig. S4). Representative single-plane confocal slices are shown in Fig. S4C.

ABCC4-mediated transport could also mediate autocrine or paracrine signaling to the small micromeres or play a role in their recruitment to the coelomic pouches (Campanale and Hamdoun, 2012). Genes with a similar profile to *ABCC4* include classic germ-line determinants *seawi, vasa,* and *ovo*, which are broadly present early and later become enriched in coelomic pouch precursor cells (CPCs) in the vegetal plate and tip of the archenteron (Juliano et al., 2006). The CPC gene regulatory network (GRN) is first initiated by *FoxY* and D/N signaling from the small micromeres, which also activates the transcription factors *foxF*, *pitx2*, *nanos* and *soxE* in the NSM (Materna et al., 2013). These genes, along with *FoxY*, stay restricted in the coelomic pouches (Juliano et al., 2006, 2010; Materna et al., 2013; Luo and Su, 2012), and thus may control *ABCC4* expression as part of the CPC GRN. A subset of transcription factors in the CPC GRN is required for the homing of small micromeres to the coelomic pouches (Martik and McClay, 2015), and may control PGC migration indirectly through the regulation of *ABCC4* expression during gastrulation. In *Drosophila*, a mesodermally-expressed ABCB ortholog is involved in the export of lipid molecules and hedgehog signaling ligands that guide PGC migration (Ricardo and Lehmann, 2009; Deshpande et al., 2016). Sphingolipids and eicosanoid-based signaling are required for PGC migration in ascidians, and ABCC transporters may play a significant role in this context (Kassmer et al., 2015, 2020).

4.2. ABCB1, B4, and G2 transporters are part of an early differentiation gene battery in gut epithelia

ABCB1 and ABCG2 have been well studied in the protection and homeostasis of enterocytes. ABCB, ABCC and ABCG transcripts and proteins are differentially regulated along the anterior-to-posterior (A/P) regions of the small and large intestines in adult mammals (Müller et al., 2017). Human ABCB1 and ABCG2 transcripts and protein have been detected in fetal enterocytes as early as 6–12 weeks of gestation (Konieczna et al., 2011; Miki et al., 2005), at which time the gut is still an undifferentiated tube. In zebrafish, an ABCB1-ortholog becomes concentrated in the intestinal bulb and larval intestine (Fischer et al., 2013). However, the transcriptional regulation of endoderm-specific ABC transporters during embryogenesis has yet to be characterized in any animal model (Han et al., 2018). This would provide insight as to

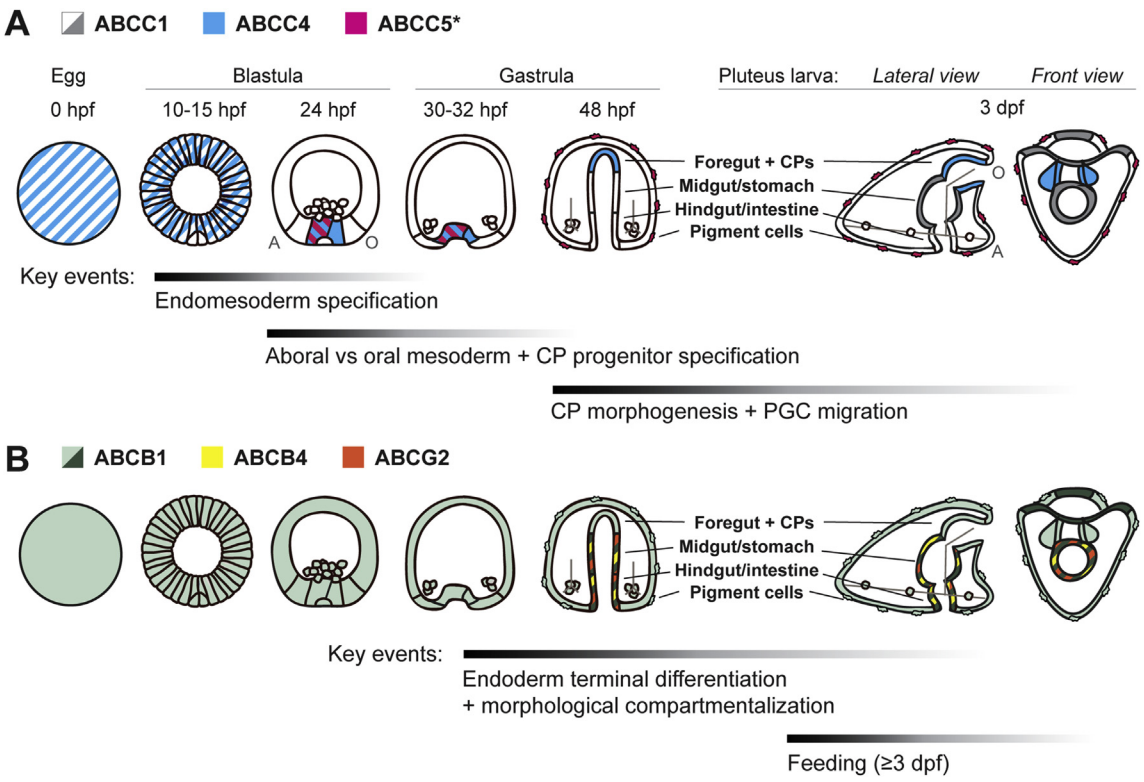

Fig. 5. Summary of ABC transporter expression and activity domains throughout embryogenesis. For each schematic, times in hours post-fertilization (hpf) or days post-fertilization (dpf) and approximate stages are shown at the top, with key developmental events indicated at the bottom. **(A) Summary of *ABCC1* (white), *ABCC4* (blue), and *ABCC5* (magenta) expression domains**. *ABCC1* appears globally expressed and becomes enriched in ectoderm and endoderm-derived sensory and feeding structures by the end of embryogenesis. In contrast, *ABCC4* exhibits ubiquitous expression in the egg and blastula, excluding the small micromeres, and then accumulates in the NSM and later expands to the mesodermally derived embryonic niche of PGCs, the coelomic pouches. The NSM domain partially overlaps with *ABCC5*, which is expressed in the aboral NSM and a subset of its derivatives, the pigment cells. Shade intensity of gray indicates the enrichment of *ABCC1* expression in certain tissues. **ABCC5* expression and efflux data are from *Shipp* et al. *(2012;2015)*. *ABCG11* is also present in pigment cells by the gastrula stage (Perillo et al., 2020). A, aboral. O, oral. CP, coelomic pouch. PGC, primordial germ cell. **(B) Summary of *ABCB1* (light green), *ABCB4* (yellow), and *ABCG2* (orange) expression domains**. Similar to *ABCC1*, transcript accumulation of *ABCB1* exhibits a ubiquitous pattern that concentrates in feeding and sensory organs post-gastrulation. In contrast, significant transcript accumulation of *ABCB4* and *ABCG2* is first present in endoderm-fated tissues of the hindgut and midgut. Shade intensity of green indicates the enrichment of *ABCB1* expression in certain tissues.

Table 4
Summary of expression domains for ABC transporters 0–72 h post fertilization.

		ABCC1	ABCC4	ABCB1	ABCB4	ABCG2
Mesoderm:	NSM	+	+++	+	-	-
	Coelomic pouches	+	+++	+	-	-
Endoderm:	Foregut	+	+	+	-	-
	Midgut	++	-	+++	+++	+++
	Hindgut	+	-	++	++	++
Ectoderm:		+	+	+	-	-
	Apical organ/ CB	++	-	+	-	-

+, relative level of expression; -, not detected in WMISH. CB, ciliary band. NSM, non-skeletal mesoderm.

when active transport becomes partitioned into the different digestive and absorptive regions of the gut.

During endoderm development, several transcription factors and signaling pathways lead to the regionalization of gut epithelial structures and compartment-specific genes along the A/P axis (Annunziata et al., 2019; Thompson et al., 2018). In our data, compartmentalization of transporters along the A/P axis of the gut was evident as early as mid-gastrulation, in cells fated to form the stomach and intestine (Fig 3; Fig 5). In the sea urchin, other gut differentiation markers are controlled by conserved *Xlox, Cdx*, and Wnt10-mediated regulatory pathways in the midgut and hindgut (Annunziata et al., 2014, 2019). It will be informative to link the endoderm GRN with *ABCB1, ABCB4* and *ABCG2* expression. Additional candidate regulators include members of the nuclear hormone receptor system, which control ABC transporter expression in terminally differentiated cells (Müller et al., 2017; Li and Wang, 2010) and are developmentally regulated in the sea urchin embryo (Goldstone et al., 2006).

4.3. Active transport domains related to gut detoxification in larvae are established prior to feeding

Our *in-situ* hybridization data show that the enrichment and co-localization of *ABCB1, B4* and *G2* genes in the gut is broadly evident across the endodermal tissue (Fig. 3). This is in contrast to genes that are specific to highly specialized cells in the stomach (*e.g*, pancreatic-like exocrine cells (Perillo et al., 2016)). The broad expression of ABC transporters within the gut is likely for protection across the whole tissue, which is evident from the observed patterns of active fluorescent substrate efflux (Fig. 4). Indeed, ABCB and ABCC activity in the cell membrane of zygotes provide protection from xenobiotics immediately following fertilization (Hamdoun et al., 2004; Bošnjak et al., 2009). Our inhibitor experiments demonstrate that this global activity persists through larval stages for the ABCB subfamily and becomes strongest in the gut (Fig. 4). While *ABCG2* expression also closely mirrors *ABCB1* orthologs in the gut, we do not yet have fluorescent substrates that give

reliable results in accumulation assays at the gastrula and larval stages.

Remarkably, the concentrated ABCB-specific transport activity in the gut is evident as early as the prism stage (Fig 4B; 54 hpf), despite the fact that feeding commences by 3 dpf. We predict that in addition to global reserves of ABCB1 across development, ABCB1, ABCB4 and ABCG2 transporters may be placed in the differentiating gut membrane early on to enable rapid detoxification capabilities as soon as the animal begins feeding. In the wild, sea urchin larvae encounter numerous harmful secondary metabolites derived from their phytoplankton-based diets (Strathmann et al., 1987; Turner and Tester, 1997). Other xenobiotic stressors include ubiquitous marine microbes, which can be commensal or pathogenic in nature (Ho et al., 2016; Schuh et al., 2020). Notably, *ABCB1* plays an important role in detoxification upon exposure to bacteria in mice and marine worms (Panwala et al., 1998; Toomey and Epel, 1993; Toomey et al., 1996). Future work in the sea urchin larva will help dissect the cross-talk between host transporters and microbial metabolism during gut development and maturation (Fleming, Schrankel et al., *in press*).

5. Conclusions

This study provides the first systematic map of SMT domains in development. The compartmentalization of gene expression across germ layers indicates that ABC transporters are under tightly regulated developmental control. This suggests that transporter activity is involved in key morphogenetic events, in addition to the metabolism or protection of specific cell types, such as the gut epithelia (Fig. 5). Collectively, these results lay the groundwork for characterizing how GRNs give rise to distinct functional territories of transport during embryogenesis. This lends insight towards the evolution of developmental functions for SMTs, and could be important for understanding how SMT activity can become recapitulated in disease settings through the reactivation of developmental pathways.

Authors' contributions

C.S.S. and A.H. conceived the study and designed experiments. C.S.S. performed the research and data analysis. C.S.S. and A.H. wrote and edited the manuscript.

Funding

This work is supported by the National Institute of Health (ES027921 and ES030318 to A.H., and F32 ES029843 to C.S.S.), and The National Science Foundation (1840844 to A.H.).

Availability of data and materials

All data generated and analyzed during this study are included in this manuscript and its supplementary information files.

Declaration of competing interest

The authors declare no competing interests.

Acknowledgements

The authors thank Dr. Victor D. Vacquier for critical reading of the manuscript. Jose Espinoza designed the WMISH primers and Travis Fleming and Himanshu Vyas assisted in larval B-ver accumulation analysis.

Appendix A. Supplementary data

Supplementary data to this article can be found online at https://doi.org/10.1016/j.ydbio.2020.12.021.

References

Ahn, S.-Y., Nigam, S.K., 2009. Toward a systems level understanding of organic anion and other multispecific drug transporters: a remote sensing and signaling hypothesis. Mol. Pharmacol. 76 (3), 481–490.
Almén, M., Nordström, K.J., Fredriksson, R., Schiöth, H.B., 2009. Mapping the human membrane proteome: a majority of the human membrane proteins can be classified according to function and evolutionary origin. BMC Biol. 7 (1), 50.
Andrikou, C., Iovene, E., Rizzo, F., Oliveri, P., Arnone, M., 2013. Myogenesis in the sea urchin embryo: the molecular fingerprint of the myoblast precursors. EvoDevo 4 (1), 33.
Andrikou, C., Pai, C.-Y., Su, Y.-H., Arnone, M.I., 2015. Logics and properties of a genetic regulatory program that drives embryonic muscle development in an echinoderm. Elife 4 e07343.
Angerer, L.M., Yaguchi, S., Angerer, R.C., Burke, R.D., 2011. The evolution of nervous system patterning: insights from sea urchin development. Development 138, 3613–3623.
Annunziata, R., Perillo, M., Andrikou, C., Cole, A.G., Martinez, P., Arnone, M.I., 2014. Pattern and process during sea urchin gut morphogenesis: the regulatory landscape. Genesis 52 (3), 251–268.
Annunziata, R., Andrikou, C., Perillo, M., Cuomo, C., Arnone, M.I., 2019. Development and evolution of gut structures: from molecules to function. Cell Tissue Res. 377 (3), 445–458, 24.
Babonis, L.S., Martindale, M.Q., 2017. Phylogenetic evidence for the modular evolution of metazoan signalling pathways. Philos Trans R Soc B Biol Sci. 372 (1713), 20150477.
Bogacheva, M.S., Khan, S., Kanninen, L.K., Yliperttula, M., Leung, A.W., Lou, Y.-R., 2018. Differences in definitive endoderm induction approaches using growth factors and small molecules. J. Cell. Physiol. 233 (4), 3578–3589.
Bošnjak, I., Uhlinger, K.R., Heim, W., Smital, T., Franekzić-Čolić, J., Coale, K., et al., 2009. Multidrug efflux transporters limit accumulation of inorganic, but not organic, mercury in sea urchin embryos. Environ. Sci. Technol. 43 (21), 8374–8380.
Burke, R.D., 1981. Structure of the digestive tract of the pluteus larva of Dendraster excentricus (Echinodermata: echinoida). Zoomorphology 98 (3), 209–225.
Butcher, R.A., 2017. Small-molecule pheromones and hormones controlling nematode development. Nature Chemical Biology. Nat Chem Biol 13, 577–586.
Campanale, J.P., Gökirmak, T., Espinoza, J.E., Oulhen, N, Wessel, G.M., Hamdoun, A.H., 2014. Migration of sea urchin primordial germ cells. Dev. Dynam. 243 (7), 917–927.
Campanale, J.P., Hamdoun, A., 2012. Programmed reduction of ABC transporter activity in sea urchin germline progenitors. Development 139 (4), 783–792.
Chen, Z.S., Tiwari, A.K., 2011. Multidrug resistance proteins (MRPs/ABCCs) in cancer chemotherapy and genetic diseases. FEBS J. 278 (18), 3226–3245.
Chen, S., Borowiak, M., Fox, J.L., Maehr, R., Osafune, K., Davidow, L., et al., 2009. A small molecule that directs differentiation of human ESCs into the pancreatic lineage. Nat. Chem. Biol. 5 (4), 258–265.
Cheung, L., Flemming, C.L., Watt, F., Masada, N., Yu, D.M.T., Huynh, T., et al., 2014. High-throughput screening identifies Ceefourin 1 and Ceefourin 2 as highly selective inhibitors of multidrug resistance protein 4 (MRP4). Biochem. Pharmacol. 91 (1), 97–108.
Cole, S.P.C., 2014 Nov. Multidrug resistance protein 1 (MRP1, ABCC1), a "multitasking" ATP-binding cassette (ABC) transporter. J. Biol. Chem. 289 (45), 30880–30888.
Davidson, E.H., Rast, J.P., Oliveri, P., Ransick, A., Calestani, C., Yuh, C.-H., et al., 2002. A genomic regulatory network for development. Science 295, 1669–1678, 5560.
Dean, M., 2001. The human ATP-binding cassette (ABC) transporter superfamily. Genome Res. 11 (7), 1156–1166.
Deshpande, G., Manry, D., Jourjine, N., Mogila, V., Mozes, H., Bialistoky, T., et al., 2016. Role of the ABC transporter Mdr49 in hedgehog signaling and germ cell migration. Dev. 143 (12), 2111–2120.
Engelhart, D.C., Azad, P., Ali, S., Granados, J.C., Haddad, G.G., Nigam, S.K., 2020. Drosophila SLC22 orthologs related to OATs, OCTs, and OCTNs regulate development and responsiveness to oxidative stress. Int. J. Mol. Sci. 21 (6), 15.
Fischer, S., Klüver, N., Burkhardt-Medicke, K., Pietsch, M., Schmidt, A.-M., Wellner, P., et al., 2013. Abcb4 acts as multixenobiotic transporter and active barrier against chemical uptake in zebrafish (Danio rerio) embryos. BMC Biol. 11 (1), 69.
Fletcher, J.I., Haber, M., Henderson, M.J., Norris, M.D., 2010. ABC transporters in cancer: more than just drug efflux pumps. Nat. Rev. Canc. 10 (2), 147–156.
Giacomini, K.M., Huang, S.-M.M., Tweedie, D.J., Benet, L.Z., Brouwer, K.L.R., Chu, X., et al., 2010. Membrane transporters in drug development. Nat. Rev. Drug Discov. 9 (3), 215–236.
Gökirmak, T., Campanale, J.P., Shipp, L.E., Moy, G.W., Tao, H., Hamdoun, A., 2012. Localization and substrate selectivity of sea urchin multidrug (MDR) efflux transporters. J. Biol. Chem. 287 (52), 43876–43883.
Gökirmak, T., Shipp, L.E., Campanale, J.P., Nicklisch, S.C.T., Hamdoun, A., 2014. Transport in technicolor: mapping ATP-binding cassette transporters in sea urchin embryos. Mol. Reprod. Dev. 81 (9), 778–793.
Goldstone, J.V., Hamdoun, A., Cole, B.J., Howard-Ashby, M., Nebert, D.W., Scally, M., et al., 2006. The chemical defensome: environmental sensing and response genes in the Strongylocentrotus purpuratus genome. Dev. Biol. 300 (1), 366–384.
Hamdoun, A.M., Cherr, G.N., Roepke, T.A., Epel, D., 2004. Activation of multidrug efflux transporter activity at fertilization in sea urchin embryos (Strongylocentrotus purpuratus). Dev. Biol. 276 (2), 452–462.
Han, L.W., Gao, C., Mao, Q., 2018. An update on expression and function of P-gp/ABCB1 and BCRP/ABCG2 in the placenta and fetus. Expet Opin. Drug Metabol. Toxicol. 14 (8), 817–829.
Hannun, Y.A., Obeid, L.M., 2008. Principles of bioactive lipid signalling: lessons from sphingolipids. Nat. Rev. Mol. Cell Biol. 9 (2), 139–150.
Helker, C.S.M., Mullapudi, S.-T., Mueller, L.M., Preussner, J., Tunaru, S., Skog, O., et al., 2019. A whole organism small molecule screen identifies novel regulators of pancreatic endocrine development, 15 Development 146 (14). dev172569.

Ho, E.C.H., Buckley, K.M., Schrankel, C.S., Schuh, N.W., Hibino, T., Solek, C.M., et al., 2016. Perturbation of gut bacteria induces a coordinated cellular immune response in the purple sea urchin larva. Immunol. Cell Biol. 94 (9), 861–874.
Jedlitschky, G., Leier, I., Buchholz, U., Barnouin, K., Kurz, G., Keppler, D., 1996. Transport of glutathione, glucuronate, and sulfate conjugates by the MRP gene-encoded conjugate export pump. Canc. Res. 56 (5), 988–994.
Jin, D., Ni, T.T., Sun, J., Wan, H., Amack, J.D., Yu, G., et al., 2014. Prostaglandin signalling regulates ciliogenesis by modulating intraflagellar transport. Nat. Cell Biol. 16 (9), 841–851.
Juliano, C.E., Stack, C., Aldrich, M., Cameron, A.R., Wessel, G.M., 2006. Germ line determinants are not localized early in sea urchin development, but do accumulate in the small micromere lineage. Dev. Biol. 300 (1), 406–415.
Juliano, C.E., Yajima, M., Wessel, G.M., 2010. Nanos functions to maintain the fate of the small micromere lineage in the sea urchin embryo. Dev. Biol. 337 (2), 220–232.
Kassmer, S.H., Rodriguez, D., Langenbacher, A.D., Bui, C., De Tomaso, A.W., 2015. Migration of germline progenitor cells is directed by sphingosine-1-phosphate signalling in a basal chordate. Nat. Commun. 6, 8565.
Kassmer, S.H., Rodriguez, D., De Tomaso, A.W., 2020. Evidence that ABC transporter-mediated autocrine export of an eicosanoid signaling molecule enhances germ cell chemotaxis in the colonial tunicate Botryllus schlosseri. Development 147 (15) dev184663.
Konieczna, A., Erdösová, B., Lichnovská, R., Jandl, M., Čížková, K., Ehrmann, J., 2011. Differential expression of ABC transporters (MDR1, MRP1, BCRP) in developing human embryos. J. Mol. Histol. 42 (6), 567–574.
Korostylev, A., Mahaddalkar, P.U., Keminer, O., Hadian, K., Schorpp, K., Gribbon, P., et al., 2017. A high-content small molecule screen identifies novel inducers of definitive endoderm. Mol Metab 6 (7), 640–650.
Li, H., Wang, H., 2010. Activation of xenobiotic receptors: driving into the nucleus. Expet Opin. Drug Metabol. Toxicol. 6 (4), 409–426. https://doi.org/10.1517/17425251003598886.
Luo, Y.-J., Su, Y.-H., 2012. Opposing nodal and BMP signals regulate left–right asymmetry in the sea urchin larva. Hamada H, editor PLoS Biol. 10 (10), e1001402, 9.
Martik, M.L., McClay, D.R., 2015. Deployment of a retinal determination gene network drives directed cell migration in the sea urchin embryo. Elife 4, e08827.
Materna, S.C., Swartz, S.Z., Smith, J., 2013. Notch and Nodal control forkhead factor expression in the specification of multipotent progenitors in sea urchin. Development 140 (8), 1796–1806.
Miki, Y., Suzuki, T., Tazawa, C., Blumberg, B., Sasano, H., 2005. Steroid and xenobiotic receptor (SXR), cytochrome P450 3A4 and multidrug resistance gene 1 in human adult and fetal tissues. Mol. Cell. Endocrinol. 231, 75–85.
Miranda, E.R., Nam, E.A., Kuspa, A., Shaulsky, G., 2015. The ABC transporter, AbcB3, mediates cAMP export in D. discoideum development. Dev. Biol. 397 (2), 203–211.
Müller, P., Rogers, K.W., Yu, S.R., Brand, M., Schier, A.F., 2013. Morphogen transport. Development 140, 1621–1638.
Müller, J., Keiser, M., Drozdzik, M., Oswald, S., 2017. Expression, regulation and function of intestinal drug transporters: an update. Biol. Chem. 398 (2), 175–192, 1.
Nakajima, Y., Burke, R.D., 1996. The initial phase of gastrulation in sea urchins is accompanied by the formation of bottle cells. Dev. Biol. 179 (2), 436–446.
Nigam, S.K., 2015. What do drug transporters really do? Nat. Rev. Drug Discov. 14 (1), 29–44.
Onjiko, R.M., Moody, S.A., Nemes, P., 2015. Single-cell mass spectrometry reveals small molecules that affect cell fates in the 16-cell embryo. Proc. Natl. Acad. Sci. Unit. States Am. 112 (21), 6545–6550.
Panwala, C.M., Jones, J.C., Viney, J.L., 1998. A novel model of inflammatory bowel disease: mice deficient for the multiple drug resistance gene, mdr1a, spontaneously develop colitis. J. Immunol. 161 (10), 5733–5744.
Pehrson, J.R., Cohen, L.H., 1986. The fate of the small micromeres in sea urchin development. Dev. Biol. 113 (2), 522–526.
Perillo, M., Wang, Y.J., Leach, S.D., Arnone, M.I., 2016. A pancreatic exocrine-like cell regulatory circuit operating in the upper stomach of the sea urchin Strongylocentrotus purpuratus larva. BMC Evol. Biol. 16 (1), 117.
Perillo, M., Oulhen, N., Foster, S., Spurrell, M., Calestani, C., Wessel, G., 2020. Regulation of dynamic pigment cell states at single-cell resolution. Elife 9 e60388.
Peter, I.S., Davidson, E.H., 2011. A gene regulatory network controlling the embryonic specification of endoderm. Nature 474 (7353), 635–639.
Randolph, G.J., Beaulieu, S., Pope, M., Sugawara, I., Hoffman, L., Steinman, R.M., et al., 1998. A physiologic function for p-glycoprotein (MDR-1) during the migration of dendritic cells from skin via afferent lymphatic vessels. Proc. Natl. Acad. Sci. U. S. A. 95 (12), 6924–6929.
Ransick, A., Rast, J.P., Minokawa, T., Calestani, C., Davidson, E.H., 2002. New early zygotic regulators expressed in endomesoderm of sea urchin embryos discovered by differential array hybridization. Dev. Biol. 246, 132–147.
Reid, G., Wielinga, P., Zelcer, N., van der Heijden, I., Kuil, A., de Haas, M., et al., 2003. The human multidrug resistance protein MRP4 functions as a prostaglandin efflux transporter and is inhibited by nonsteroidal antiinflammatory drugs. Proc. Natl. Acad. Sci. U. S. A. 100 (16), 9244–9249.
Ricardo, S., Lehmann, R., 2009. An ABC transporter controls export of a Drosophila germ cell attractant. Science 323 (5916), 943–946.
Robert, H.S., Friml, J., 2009. Auxin and other signals on the move in plants. Nat. Chem. Biol. 5 (5), 325–332.
Rosenthal, S.B., Bush, K.T., Nigam, S.K., 2019. A network of SLC and ABC transporter and DME genes involved in remote sensing and signaling in the gut-liver-kidney Axis. Sci. Rep. 9 (1), 11879.
Schindelin, J., Arganda-Carreras, I., Frise, E., Kaynig, V., Longair, M., Pietzsch, T., et al., 2012. Fiji: an open-source platform for biological-image analysis. Nat. Methods 9 (7), 676–682.
Schrankel, C.S., Solek, C.M., Buckley, K.M., Anderson, M.K., Rast, J.P., 2016. A conserved alternative form of the purple sea urchin HEB/E2-2/E2A transcription factor mediates a switch in E-protein regulatory state in differentiating immune cells. Dev. Biol. 416 (1), 149–161.
Schuh, N.W., Carrier, T.J., Schrankel, C.S., Reitzel, A.M., Heyland, A., Rast, J.P., 2020. Bacterial exposure mediates developmental plasticity and resistance to lethal Vibrio lentus infection in purple sea urchin (Strongylocentrotus purpuratus) larvae. Front. Immunol. 10, 3014.
Shipp, L.E., Hamdoun, A., 2012. ATP-binding cassette (ABC) transporter expression and localization in sea urchin development. Dev. Dynam. 241 (6), 1111–1124.
Shipp, L.E., Hill, R.Z., Moy, G.W., Gökirmak, T., Hamdoun, A., 2015. Abcc5 is required for cAMP-mediated hindgut invagination in sea urchin embryos. Dev. 142 (20), 3537–3548.
Solek, C.M., Oliveri, P., Loza-Coll, M., Schrankel, C.S., Ho, E.C.H., Wang, G., et al., 2013. An ancient role for Gata-1/2/3 and Scl transcription factor homologs in the development of immunocytes. Dev. Biol. 382 (1), 280–292.
Strathmann, R.R., 1987. Larval feeding. In: Giese, A.C., Pearse, J.S., Pearse, V.B. (Eds.), Reproduction of Marine Invertebrates Volume IX: General Aspects: Seeking Unity in Diversity. Blackwell Sci. Publ., Palo Alto/Boxwood Press, Pacific Grove, CA, pp. 465–550.
Szakács, G., Váradi, A., Özvegy-Laczka, C., Sarkadi, B., 2008. The role of ABC transporters in drug absorption, distribution, metabolism, excretion and toxicity (ADME-Tox). Drug Discov. Today 13 (9–10), 379–393.
Thompson, C.A., DeLaForest, A., Battle, M.A., 2018. Patterning the gastrointestinal epithelium to confer regional-specific functions. Dev. Biol. 435 (2), 97–108.
Titus, M.A., Goodson, H.V., 2018. Developing evolutionary cell biology. Dev. Cell 47 (4), 395–396.
Toomey, B.H., Epel, D., 1993. Multixenobiotic resistance in urechis caupo embryos: protection from environmental toxins. Biol. Bull. 185 (3), 355–364.
Toomey, B.H., Kaufman, M.R., Epel, D., 1996. Marine bacteria produce compounds that modulate multixenobiotic transport activity in Urechis caupo embryos. Mar. Environ. Res. 42 (1–4), 393–397.
Tu, Q., Cameron, R.A., Davidson, E.H., 2014. Quantitative developmental transcriptomes of the sea urchin Strongylocentrotus purpuratus. Dev. Biol. 385 (2), 160–167.
Turner, J.T., Tester, P.A., 1997. Toxic marine phytoplankton, zooplankton grazers, and pelagic food webs. Limnol. Oceanogr. 42 (5), 1203–1213.
van Aubel, R., 2002. A MH, Smeets PHE, Peters JGP, Bindels RJM, Russel FGM. The MRP4/ABCC4 gene encodes a novel apical organic anion transporter in human kidney proximal tubules: putative efflux pump for urinary cAMP and cGMP. J. Am. Soc. Nephrol. 13 (3), 595–603.
Wada, H., Satoh, N., 1994. Phylogenetic relationships among extant classes of echinoderms, as inferred from sequences of 18S rDNA, coincide with relationships deduced from the fossil record. J. Mol. Evol. 38 (1).
Wen, J., Luo, J., Huang, W., Tang, J., Zhou, H., Zhang, W., 2015. The pharmacological and physiological role of multidrug-resistant protein 4. J. Pharmacol. Exp. Therapeut. 354 (3), 358–375.
Wielinga, P.R., van der Heijden, I., Reid, G., Beijnen, J.H., Wijnholds, J., Borst, P., 2003. Characterization of the MRP4- and MRP5-mediated transport of cyclic nucleotides from intact cells. J. Biol. Chem. 278 (20), 17664–17671.
Wijnholds, J., Mol, C.A.A.M., van Deemter, L., de Haas, M., Scheffer, G.L., Baas, F., et al., 2000. Multidrug-resistance protein 5 is a multispecific organic anion transporter able to transport nucleotide analogs. Proc. Natl. Acad. Sci. Unit. States Am. 97 (13), 7476–7481.
Yabe, T., Suzuki, N., Furukawa, T., Ishihara, T., Katsura, I., 2005. Multidrug resistance-associated protein MRP-1 regulates dauer diapause by its export activity in Caenorhabditis elegans. Development 132 (14), 3197–3207.
Yanes, O., Clark, J., Wong, D.M., Patti, G.J., Sánchez-Ruiz, A., Benton, H.P., et al., 2010. Metabolic oxidation regulates embryonic stem cell differentiation. Nat. Chem. Biol. 6 (6), 411–417.
Zúñiga, A., Hödar, C., Hanna, P., Ibáñez, F., Moreno, P., Pulgar, R., et al., 2009. Genes encoding novel secreted and transmembrane proteins are temporally and spatially regulated during Drosophila melanogaster embryogenesis. BMC Biol. 7 (1), 61.

Glossary

ABC: ATP-binding cassette
B-ver: BODIPY-Verapamil
CB: ciliary band
CPs: coelomic pouches
CF: Ceefourin
Dpf: days post-fertilization
Fg: foregut
FDA: fluorescein diacetate
FISH: fluorescent *in-situ* hybridization
GRN: gene regulatory network
Hg: hindgut
Hpf: hours post-fertilization
MDR: multidrug resistance
Mg: midgut
MRP: multidrug resistance protein
NSM: non-skeletal mesoderm
PGC: primordial germ cell
SLC: solute-carrier
SMM: small micromeres
WMISH: whole mount *in-situ* hybridization